Preponderance of Late-spiking Neurons in Rat Lateral Amygdala.

Ewan C. McNay[1] and Thomas H. Brown

Department of Psychology, Yale University, New Haven CT 06520

Whole-cell recordings from rat lateral amygdala (LA) revealed two populations of principal neurons, that have similar pyramid-like morphologies but differing in firing pattern: late-spiking (LS, 66%) and regular-spiking (RS, 34%). The presence of large numbers of LS neurons arguably supports recent suggestions that the LA should be considered to be a functional extension of perirhinal cortex.

The lateral amygdala has been the focus of continued interest, due in large part to its role in fear conditioning (Pitkänen et al., 1997). Recently, Swanson has suggested that the amygdala should not be considered as a structural and functional unit; indeed, that the amygdalar nuclei should be considered as individual entities (Swanson and Petrovich, 1998; Swanson, 2000). In particular, the lateral and anterior basolateral nuclei are suggested to be an extension of the overlying cortex. Studies in our laboratory have recently characterized the perirhinal cortex (PR), which largely overlies the lateral amygdala (Beggs et al., 2000; McGann et al., 2001; Moyer et al., 2001). These studies have shown that one unique feature of the PR is the presence of large numbers of late-spiking (LS) neurons in all cortical layers from II through VI.

LS neurons have also been seen in amygdalar nuclei adjacent to LA (Washburn and Moises, 1992; Martina et al., 1999), and indeed they predominate in the central amygdala (CEA), although the exact firing properties of LS neurons in CEA differ from those found in PR (Martina et al., 1999). The response characteristics of LS neurons are especially relevant to determining the role of the LA in amygdalar information processing, as delay in response to synaptic stimulation (Beggs et al., 2000) may permit such neurons to have a key role in encoding temporal relationships among stimuli, and hence in response learning (Tieu et al., 1999; McGann and Brown, 2000).

Surprisingly, given the import of the LA, only recently has an extensive attempt been made to detail the electrophysiological properties of LA neurons (Faber et al., 2001). In this comprehensive study, whole-cell patch-clamp data from 252 LA neurons were reported, and the cells classified in terms of their degree of adaptation during depolarizing current injection. *The authors reported finding no LS cells*, but rather a range of cells of a type that we have previously classified as regular-spiking (RS; McGann et al., 2001; Moyer et al., 2001). However, several features of the Faber et al. study suggest that the presence of LS cells in the LA may have been overlooked as a consequence of the methods used. In particular, Faber et al. used current steps of short duration (600 ms) and large amplitude (a minimum of 100 pA, increasing in further 100 pA increments).

Based on our work in PR, showing that the threshold level for action potential (AP) generation in PR LS neurons is well below 100 pA (McGann et al., 2001; Moyer et al., 2001), and that such cells may take several seconds to produce APs following near-threshold depolarization, we hypothesized that LS neurons in the LA might have incorrectly appeared to be RS neurons because of the methods used by Faber et al. (2001). Here we show that when depolarizing pulses of smaller amplitude and longer duration are used, allowing LS behavior to be observed, the LA is seen to contain more than 60% LS neurons, supporting both our

[1] Corresponding author. Email correspondence to ewan.mcnay@yale.edu.

hypothesis and Swanson's suggestion that the LA should be considered as a functional and developmental extension of PR.

Methods

Coronal brain slices were prepared essentially as previously described for horizontal brain slices (Moyer and Brown, 1998; Moyer et al., 2001), in ice-cold sucrose-CSF (composition in mM: 206 sucrose, 1 $CaCl_2$, 1 $MgCl_2$, 2 $MgSO_4$, 1.25 NaH_2PO_4, 26 $NaHCO_3$, 10 D-glucose) using a temperature-controlled vibratome. Slices were allowed to recover for ~1 hour of recovery at room temperature (23-25 °C) in oxygenated artificial CSF (composition in mM: 124 NaCl, 2.8 KCl, 2 $CaCl_2$, 2 $MgSO_4$, 1.25 NaH_2PO_4, 26 $NaHCO_3$, 10 D-glucose, pH 7.4, 295mOsmol). Whole-cell recordings were made between 26 and 28 °C using IR-DIC visualization of primary neurons in rat lateral amygdala. Cells were located 89.5 ± 2.1 μm below the slice surface (range: 60 to 120 μm). All recordings were somatic, and were analyzed only if the cell had an uncorrected resting membrane voltage more negative than –60 mV (voltages were corrected for a measured +13 mV liquid junction potential) and overshooting action potentials of at least 70 mV from threshold. Patch pipettes (resistance 3.1 ± 0.1 MΩ) were made from borosilicate glass and filled with 0.5% biocytin recording solution (in mM: 120 K-gluconate, 1.0 EGTA, 20 KCl, 2.0 $MgCl_2$, 2.0 Na_2•ATP, 0.25 Na_3•GTP, pH 7.3, 290 mOsmol). Pipette tips were fire polished using a Narashige microforge. Data were analyzed both on- and off-line using custom software written in IgorPro. Reconstructions of biocytin-filled neurons were obtained as previously described (Faulkner and Brown, 1999). Neuronal input resistance (R_N) was calculated from the slope of the least-squares regression line through the early, linear portion of the V-I relationship near resting potential and measured at ~5s after current onset, well into steady state. The firing

Table 1. Comparisons between primary cell types in rat LA.

Property measured	Units	Overall (n=41)	LS cells (n=27)	RS cells (n=14)
Resting membrane potential	mV	-75.23 ± .30	-75.8 ± .40	-74.16 ± .45*
Input resistance at 4950 ms	MΩ	359.24 ± 16.55	359.75 ± 21.42	358.25 ± 26.42
Time constant	ms	80.90 ± 3.27	80.285 ± 3.45	82.50 ± 6.72
AP amplitude	mV	80.86 ± 1.35	82.023 ± 1.77	78.61 ± 1.95
AP width at half-height	ms	2.40 ± .08	2.45 ± .12	2.31 ± .10
AP rise:fall dV/dt ratio		3.55 ± .10	3.60 ± .13	3.45 ± .13
Threshold for AP generation	mV	-45.69 ± .57	-45.78 ± .75	-45.51 ± .87
Maximum latency to AP	ms	2387.64 ± 312.86	3430.76 ± 324.09	375.92 ± 64.12§

* indicates a statistically significant difference between LS and RS cells at the .05 level, § at the .000001 level, determined by unpaired t-tests. t(39) = 2.38 for comparison of resting membrane potential, t(39) = 6.71 for comparison of maximum latency.

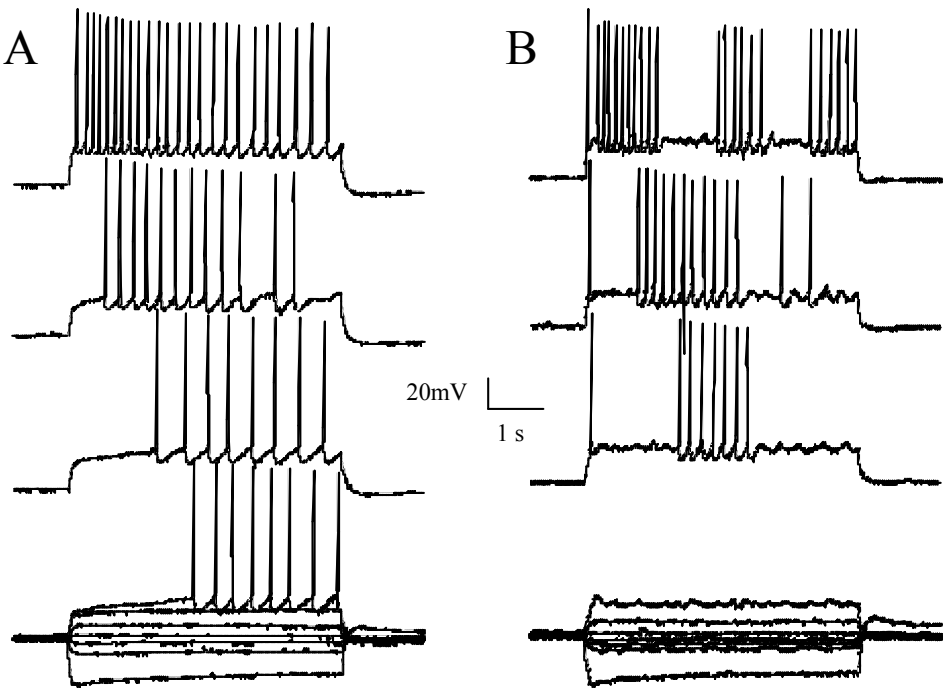

A: Series of representative voltage traces from a LS neuron. Amount of depolarizing current is progressively greater in higher traces. Note slow ramp of depolarization, especially evident in lower two traces. B: Series of representative voltage traces from a RS neuron, as in A. Note the oscillations in resting membrane voltage just below threshold (bottom trace) and above threshold (high traces)

pattern of each cell was determined using alternating de- and hyper-polarizing 5 second current injections with roughly 5 pA increments, and then iterating near threshold in increments of ~1 pA.

Results

Physiology. Analysis of firing patterns revealed two distinct populations of neurons: late-spiking (LS; 27/41 or 66%) and regular-spiking (RS 14/41 or 34%), following the terminology used in our characterization of PR (McGann et al., 2001). LS neurons were characterized by a two-stage response to depolarizing current injections near threshold: an initial, rapid rise followed by a slow ramp, which led to an AP if the injection was supra-threshold. In contrast, RS neurons showed no such ramp, and consequently had much lower maximum latencies to spike.

Table 1 details the cells' electrophysiological characteristics, both as a pooled population and broken down by cell type. As would be expected, the two cell types differed significantly in maximum latency to spike, but a significant – though small - difference was also observed in resting membrane potential (mean of –74.16 mV for RS cells vs. –75.79 for LS cells; $t(39) = 2.38$, $p<0.05$). The two cell types did not differ on any other variable measured. Representative

series of voltage traces from one RS and one LS neuron are shown in Figure 1; the slow ramp and long latency to fire of the LS neuron can clearly be seen. Interestingly, a majority of the RS

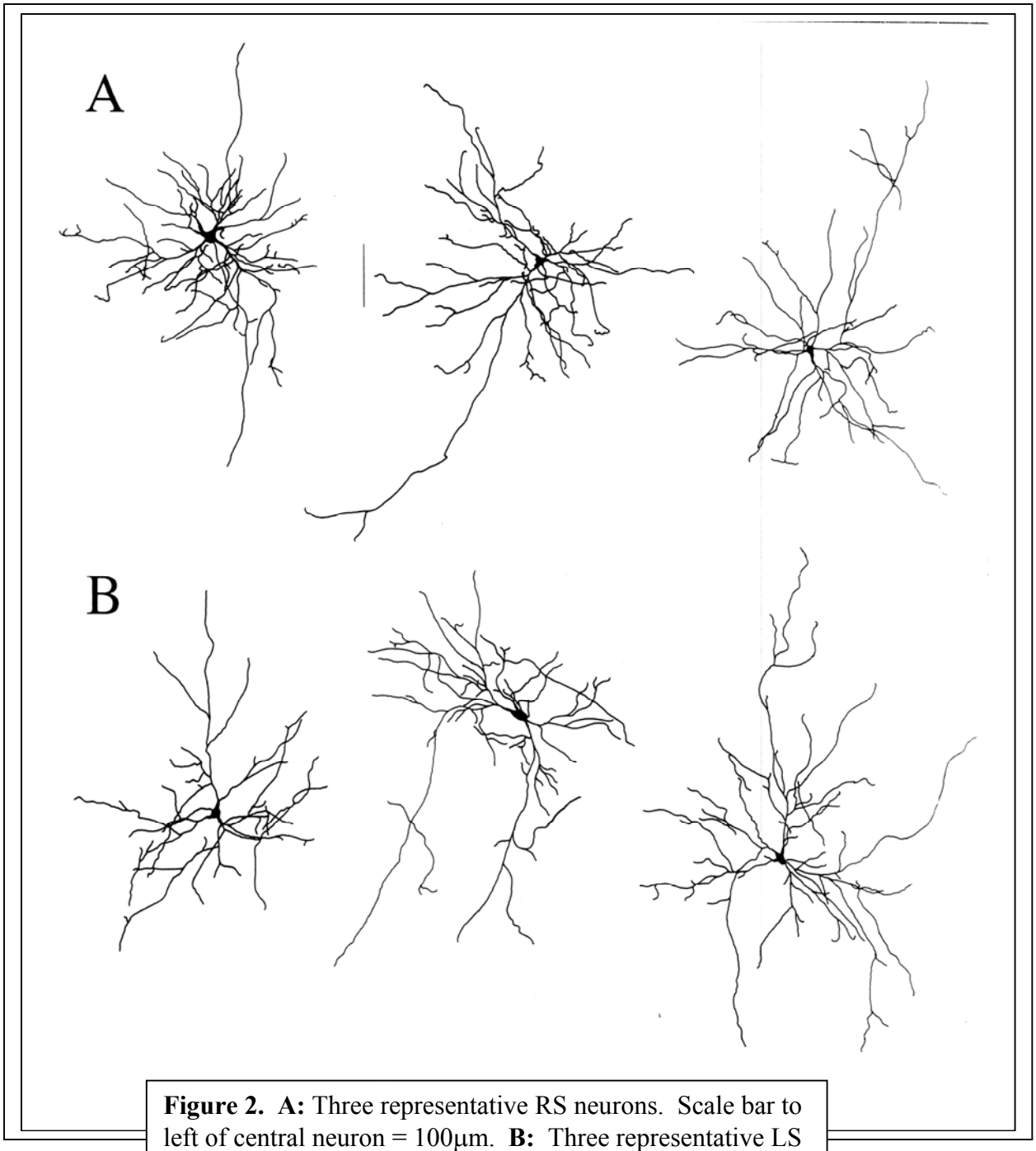

Figure 2. A: Three representative RS neurons. Scale bar to left of central neuron = 100μm. **B:** Three representative LS neurons, same scale. All neurons analysed were spiny throughout their dendritic arbors, and individual spines are hence not shown.

neurons (10/14, or 70%) showed oscillations in resting membrane potential such as have recently been described in recordings from cat lateral amygdala (Paré et al., 1995). Figure 1 shows an example of such an oscillating neuron. None of the LS neurons from which we recorded showed

such oscillations. Both LS and RS neurons responded to depolarizing current injections significantly above threshold by producing a stream of APs that continued for the duration of the current injection.

Morphology. The use of IR-DIC visualization allowed us to target principal neurons. Success was confirmed both by the lack of fast-spiking (FS) cells, believed to be interneurons, in the recordings and by the biocytin reconstructions obtained, none of which was of the small, aspiny type which we have previously found (McGann et al., 2000) to be indicative of such interneurons. Given the difficulties of determining pyramidal vs. non-pyramidal morphology from a two-dimensional reconstruction, we follow the literature in noting merely that all reconstructed cells were spiny, with morphology similar to that termed pyramid-like (Faber et al., 2001) or multipolar (Paré et al., 1995). Representative examples of reconstructed LS and RS neurons are shown in Figure 2. As in PR, there do not appear to be obvious distinguishing characteristics by which one can predict whether a given LA neuron will exhibit LS or RS firing behavior. There was no clear pattern to the location of LS versus RS neurons, with both types scattered throughout the LA.

Discussion

We hypothesized that characterizing LA neurons using near-threshold depolarizing current injections would reveal the presence of late-spiking neurons - in contrast to the report of Faber et al. (2001). This hypothesis was confirmed, in that 66% of neurons in the LA were found to be LS. This finding supports the suggestions of Swanson and colleagues (Swanson and Petrovich, 1998; Swanson, 2000) that LA should be considered an extension of PR, as one of the defining characteristics of PR vs. other areas of cortex is the presence of large numbers of LS neurons at all layers (Beggs et al., 2000; McGann et al., 2001; Moyer et al., 2001). Moreover, the properties of the LS neurons reported here are very similar to those reported for LS neurons in layers V and VI of the PR (McGann et al., 2001; Moyer et al., 2001). LS neurons in LA and PR show similar morphology, with no clear distinguishing characteristics.

Faber et al. (2001) suggested that their failure to find LS cells in the LA differed from preliminary findings from this laboratory (Faulkner and Brown, 1999) due to the presence of calcium chelators in the recording solution used by Faulkner and Brown (and also used here) and their effects on after-hyperpolarization (AHP). The difference in recording solution seems a plausible cause of the differences seen in accommodation: a large majority of the neurons reported by Faber et al. fired only between two and five spikes, even in response to very large current injections, while we do not see such marked adaptation. However, as the key characteristic of LS cells is the delay to firing their first AP, rather than their adaptation behavior, differences in AHP seem unlikely to affect LS behavior. Rather, we suggest that the 100 pA-increment current injections used by Faber et al. are likely to have obscured LS behavior. This suggestion is supported by our observations (not shown) that 100 pA injections into a subset of the LS neurons analyzed here produced spike trains that closely resembled those reported by Faber et al., with relatively short delays to the first AP. Differences in protocol may also explain the fact that the time constant (tau) we report in Table 1 is much larger than that reported by Faber and colleagues (2001). We calculated tau from the response to small (5-10 pA) current injections, which produce no overshoot of hyperpolarization and reflect only passive membrane properties.

The present data support suggestions that, both structurally and functionally, the LA can usefully be considered as an extension of the overlying PR, and that the role of both in

information processing and mediating responses to fear may depend upon the temporal response characteristics of LS neurons. In particular, LS neurons may act as essential elements of encoding time at several stages within the LA-PR circuitry involved in fear conditioning.

References.

Beggs, J. M., Moyer, J. R. Jr., McGann, J. P. and Brown, T. H. (2000) Prolonged synaptic integration in perirhinal cortical neurons. *J. Neurophysiol.*, **83**, 3294-3298.

Faber, E. S. L., Callister, R. J. and Sah, P. Morphological and Electrophysiological properties of principal neurons in the rat lateral amygdala in vitro. *J. Neurophysiol.* **85**, 714-723.

Faulkner, B. and Brown, T. H. (1999) Morphology and physiology of neurons in the rat perirhinal-lateral amygdala area. *J. Comp. Neurol.*, **411**, 613-642.

Martina, M., Royer, S. and Paré, D. (1999) Physiological properties of central medial and central lateral amygdala neurons. *J. Neurophysiol.* **82**, 1843-1854.

McGann, J. P. and Brown, T. H. (2000) Fear conditioning model predicts key temporal aspects of conditioned response production. *Psychobiology*, **28**, 303-313.

McGann, J. P., Moyer, J. R. Jr. and Brown, T. H. (2001) Predominance of late-spiking neurons in layer VI of rat perirhinal cortex. *J. Neuroscience*. **21**, 4969-76.

Moyer, J. R. Jr. and Brown, T. H. (1998) Methods for whole-cell recording from visually preselected neurons of perirhinal cortex in brain slices from young and aging rats. *J. Neurosci. Meth.* **86**, 35-54.

Moyer, J. R. Jr., McNay, E. C. and Brown, T. H. (2002) Three classes of pyramidal neurons in layer V of rat perirhinal cortex. *Hippocampus*. **12**, 218-34.

Paré, D., Pape, H.-C. and Dong, J. (1995) Bursting and Oscillating neurons of the cat basolateral amygdaloid complex in vivo: electrophysiological properties and morphological features. *J. Neurophysiol.*, **73**, 1179-1191.

Pitkänen, A., Savander, V. and LeDoux, J. E. (1997) Organization of intra-amygdaloid circuitries in the rat: an emerging framework for understanding functions of the amygdala. *Trends Neurosci.*, **20**, 517-523.

Swanson, L. W. (2000) Cerebral hemisphere regulation of motivated behavior. *Brain Res.*, **886**, 113-164.

Swanson, L. W. and Petrovich, G. D. (1998) What is the amygdala? *Trends Neurosci.*, **21**, 323-331.

Tieu, K. H., Kiedel, A. L., McGann, J. P., Faulkner, B. and Brown, T. H. (1999) Perirhinal-amygdala circuit-level computational model of temporal encoding in fear conditioning. *Psychobiology*, **27**, 1-25.

Washburn, M. S. and Moises, H. C. (1992) Electrophysiological and morphological properties of rat basolateral amygdaloid neurons in vitro. *J. Neurosci.,*, **12**, 4066-4079.